



**THEORETICAL VALIDATION AND DESIGN APPLICATION
OF MSC/NASTRAN
SNAP-THROUGH BUCKLING CAPABILITY**

Dr. M.M. Moharir
Consulting Staff Engineer, Dept. 530
The Aerostructures Corporation
1431 Vultee Boulevard
Nashville, TN 37217

Abstract

MSC/NASTRAN's Snap-Through Buckling capability is validated using a closed form solution based on the large displacement theory and the nonlinear eigenvalue extraction procedure for flat and "slightly" curved thin plates. Excellent correlation is observed for displacements, stresses, and buckling loads at Snap-Through. The capability is used to design and analyze the leading edge of a large commercial airplane.

TABLE OF CONTENTS

1. INTRODUCTION.....	3
2. THEORETICAL BACKGROUND OF NONLINEAR BUCKLING.....	3
2.1 Eigenvalue Problem.....	3
2.2 Large Displacement Theory of Curved Plates.....	4
2.3 NASTRAN Numerical Algorithm.....	4
3. NASTRAN TEST CASES.....	5
3.1 Test Structure 1.....	5
3.2 Test Structure 2.....	6
3.3 Test Structure 3.....	6
3.4 NASTRAN Runs on Test Structure 1.....	6
3.4.1 Newton's Method.....	6
3.4.2 Newton's Method With Small Increments.....	6
3.4.3 Crisfield's Arc-Length Method.....	6
3.4.4 Crisfield's Method with Small Increments.....	7
3.4.5 Analysis at The Snap-Through Jump.....	7
3.5 NASTRAN Runs on Test Structure 2.....	8
3.6 NASTRAN Run on Test Structure 3.....	9
4. PRACTICAL APPLICATION OF NASTRAN.....	10
4.1 The Leading Edge Structure.....	10
4.2 Finite Element Model.....	11
4.3 Analysis Results.....	12
5. CONCLUSIONS AND RECOMMENDATIONS.....	15

LIST OF FIGURES

Figure 1: Simply Supported Convex Plate.....	4
Figure 2: Crisfield's Arc-Length Method.....	5
Figure 3: NASTRAN Results Compared with ESDU Example.....	7
Figure 4: Post-Buckling Analysis by Crisfield's Arc-Length Method.....	8
Figure 5: Structural Elements of a Leading Edge.....	11
Figure 6: Nonlinear Buckling Analysis of L/E and D-Nose Section Between TR7 and TR8.....	12
Figure 7: Displacement Fringes of Top Skin Between TR7 and TR8.....	13
Figure 8: Finite Element Model of L/E and D-Nose Section Between TR15 and TR17.....	13
Figure 9: Nonlinear Buckling Analysis of L/E and D-Nose Section Between TR15 and TR17.....	14
Figure 10: Displacement Fringes of Top Skin Between TR15 and TR17.....	14

1. INTRODUCTION

Curved plates or flat plates with initial imperfections can exhibit a special behavior in which a large change in deflection takes place with a small change in load increment. This “snap-through” jump in deflection occurs from the side of initial curvature to the other side of the supports. When small increments of load are applied to the plate, the middle surface compressive stress builds up and then suddenly releases the internal strain energy in the form of external work done, causing the snap-through jump. The phenomenon may be reversible with a small decrement in load, resulting in a “snap-back” condition. In the current study, material nonlinearity is not involved, and therefore it is assumed that, if NASTRAN can analyze a snap-through jump, it will work for a snap-back condition also.

The snap-through jump is generally accompanied by both numerical and structural instabilities. The latter results in a buckled structure. Numerical instability warrants a special analytical procedure in the vicinity of the snap-through. Also, the deflection may decrease at the critical load increments resulting in a singular stiffness matrix.

A general theoretical background of nonlinear buckling is summarized in Section 2.1. Information on the large displacement theory used in validating NASTRAN is presented in Section 2.2. The NASTRAN numerical algorithm and critical comments are in Section 2.3. Three cases are selected to validate the MSC/NASTRAN snap-through buckling capability. A brief description of each case is given in Sections 3.1 through 3.3. NASTRAN test runs and the comparison of their results with the theory are in Sections 3.4 through 3.6. After validating the snap-through buckling capability, NASTRAN is used to analyze the Leading Edge of a large commercial airplane. The subsequent sections deal with this analysis.

2. THEORETICAL BACKGROUND OF NONLINEAR BUCKLING

2.1 Eigenvalue Problem

Nonlinear buckling analysis of a structure is an eigenvalue problem whose equation can be written as:

$$(K_n + K) [U] = [0] \quad (2.1)$$

where

$$K = K_n - K_{n-1}$$

and n and $(n - 1)$ are the two consecutive solution steps selected by the user in the vicinity of instability to update the stiffness matrices K_n and K_{n-1} . Eigenvalues are approximate if the selected value of n is away from the instability. The customary eigenvectors are $[U]$.

NASTRAN computes the increment of displacement vector:

$$(\Delta U) = (U_n) - (U_{n-1})$$

The load increment is:

$$(\Delta P) = (P_n) - (P_{n-1}) \quad (2.2)$$

Using the principle of virtual work, NASTRAN computes:

$$= \frac{(\Delta U)^T (K_n + K) (\Delta U)}{(\Delta U)^T (\Delta P)} \quad (2.3)$$

The critical buckling load is estimated as:

$$(P_{cr}) = (P_n) + (\Delta P) \quad (2.4)$$

NASTRAN prints values for the computed modes. Implementation of Equation 2.4 is tested in Section 3 of this paper for various boundary conditions of flat and curved plates having a tendency for snap-through buckling.

2.2 Large Displacement Theory of Curved Plates

It is essential to use Large Displacement Theory when the plate deflections are no longer small compared to the thickness of the plate. The formulation should account for a strain at the middle plane of the plate. A closed form solution of this problem is summarized in two simultaneous fourth order partial differential equations, equations (245) and (246) of [1]. For ease in applying these equations, [2] uses curved plates with an initial shape of the double sine curves shown in Figure 1, below. The loads are of uniform intensity. The follower forces are not accounted for. The forces remain normal to the *initial* curved surface of the plate. The solutions of these equations for square plates are given in [2] covering simply supported and fixed edges of the plate. Parametric curves are available for stresses and deflections at the key locations, such as at the center and edges of the plate.

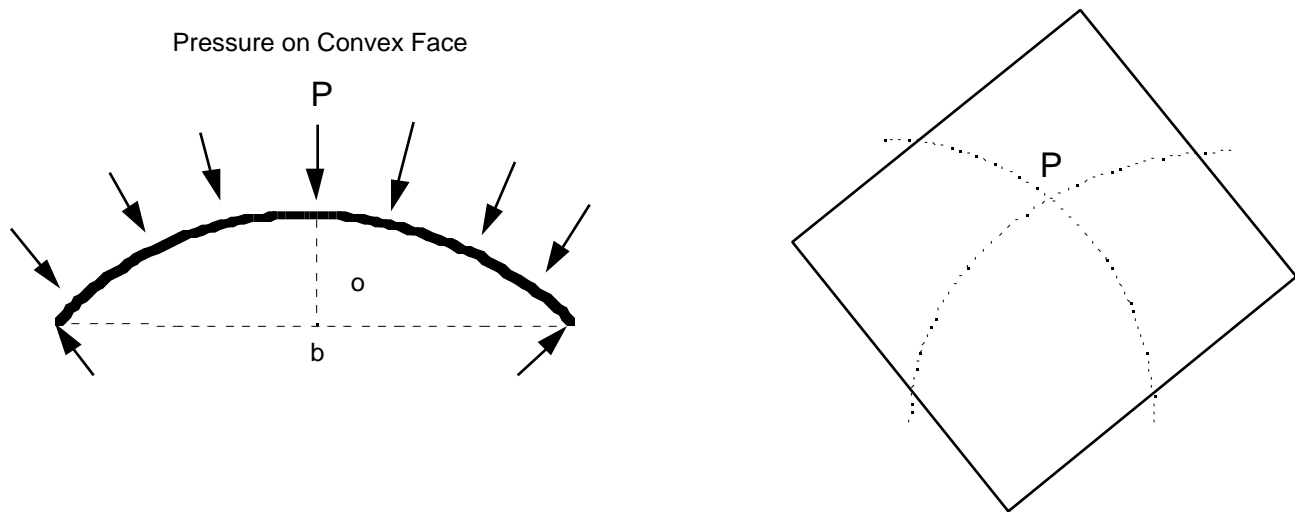


Figure 1: Simply Supported Convex Plate

2.3 NASTRAN Numerical Algorithm

In practical designs, engineers want to know the factor of safety of the structure for a nonlinear buckling load. Post-buckling analysis is required in such situations. The conventional Newton's method fails because of the singularity of the stiffness matrix and a diverging solution. In general, the Arc-Length methods avoid this situation and help to continue the analysis beyond the buckling load. In order to duplicate the theoretical values of the snap-through jump P-Delta curves, post-buckling analysis in the vicinity of the jump should be carried out with small load increments.

A typical Arc-Length Method, such as Crisfield's, specifies increments in terms of an arc of a load-displacement curve. Consider a subcase going from load 0 to load P: the Crisfield algorithm tries to use a user specified load increment (say from 0 to P_i) as follows:

$$P_i = \mu_i P \text{ where } 0 < \mu_i < 1.0$$

The 0 to P_i load increment will not be attempted directly but needs to go in subincrements due to singularity.

$$\mu = \mu_i - \mu_{i-1}$$

The required surface curvature of the plate is obtained by the linear analysis of a uniformly loaded flat plate simply supported at the edges. The load magnitude is adjusted such that the central deflection is 0.096 inch. This deflected shape becomes the initial curved surface of TS1.

3.2 Test Structure 2

Test Structure 2 (TS2) has the same sectional and material properties as TS1, except that TS2 is a flat plate, fully fixed at all the edges.

3.3 Test Structure 3

Test Structure 3 (TS3) is selected to check the utility of the deflection and stress curves of [2] for a practical aircraft panel which invariably has a curved surface and curved edges. The initial curved surface and the curved edges are generated by the linear run of a flat square plate fixed only at the corners but free at all the edges. The edges of TS3 are simply supported. The undeformed shape of TS3 is the deformed shape of the above described flat plate. The load is adjusted to give a central deflection of 0.096 inch. The corresponding central edge deflection is 0.0615 inch, giving the initial bow at the center of plate $\delta_0 = (0.096 - 0.0615) = 0.0345$ inch.

3.4 NASTRAN Runs on Test Structure 1

3.4.1 Newton's Method

TS1 is analyzed by making a series of runs using the conventional Newton's method of iteration. In one of the runs the pressure of 10 psi is given 10 increments of 1 psi each. NASTRAN results duplicate the theoretical deflection results over the 10 psi range, except between 1 and 2 psi where the snap-through jump occurs. The NASTRAN results are within 3 percent of the theoretical deflections and stresses. For example, Curve 6 of [2], which is based on Large Displacement Theory, gives a maximum stress occurring at the center of the plate of 28,210 psi. NASTRAN prints the value 28,950 psi for a 10 psi pressure. Curve 5 of [2] yields a deflection of 0.2319 inch, whereas NASTRAN prints 0.2327 inch at the center of the plate.

3.4.2 Newton's Method With Small Increments

In the second type of run for Newton's method, subcase 1 has 1.45 psi pressure and subcase 2 has 1.85 psi pressure with 40 increments of 0.01 psi each. NASTRAN bombs out at the twenty-ninth iteration because of two diverging solutions. The presence of a buckling mode is detected at this location. Thus, the predicted buckling load is in the vicinity of $1.45 + .01(29-1) = 1.73$ psi.

The theoretical buckling load given in [2] is 1.57 psi. The difference can be attributed to the fact that the theory does not account for the follower forces as stated in Section 2.2. Also, it is observed that the solution is very sensitive to numerical accuracy in this region of the P-Delta curve. Since the conventional Newton's method fails near the snap-through jump where instability occurs, no eigenvalue analysis is possible for this buckling mode.

3.4.3 Crisfield's Arc-Length Method

A series of test runs are made using Crisfield's Arc-Length method. Subcase 1 has 2 psi pressure in 20 equal increments. The solution converges at a 0.8626 psi load factor before a buckling mode is detected. The next load factor is 0.8691 psi. Therefore, the critical load factor is between 0.8626 psi and 0.8691 psi. The average load factor is 0.8658 psi, which gives a critical load of approximately 1.731 psi (Initial load $0 + 0.8658 \times 2$). The exact value is obtained by the next series of eigenvalue extraction restart runs. It is further shown in Figure 3 that the P-Delta curves for the theory, Crisfield's method and the conventional

Newton's method, are almost identical, with the exception that the conventional method fails near the snap-through jump as mentioned in Section 3.4.2.

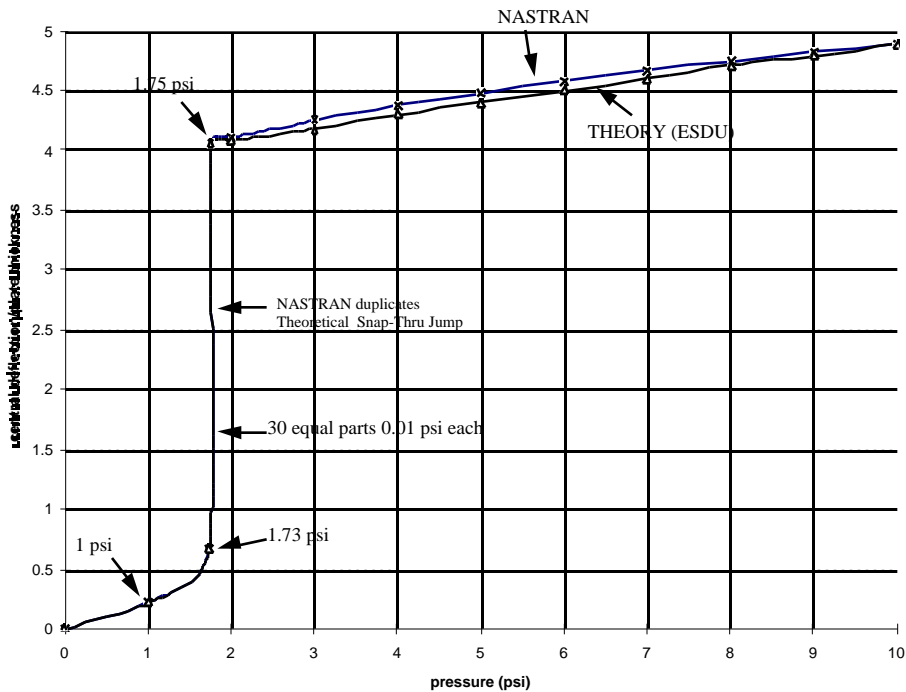


Figure 3: NASTRAN Results Compared with ESDU Example

3.4.4 Crisfield's Method with Small Increments

The initial run has one subcase. The load is 1.7 psi with 5 increments. It uses Crisfield's Arc-Length method. The restart run is from the last "loopid" of the initial run. Twenty increments are used between 1.7 and 1.8 psi. The eigenvalue extraction procedure starts just after the load of 1.709 psi. Using equation (2.4) of Section 2 the critical load is

$$\begin{aligned}
 P_{cr} &= 1.709 + (3.128 \times .005) \\
 &= 1.725 \text{ psi}
 \end{aligned}$$

3.4.5 Analysis at The Snap-Through Jump

This test run, with twenty four subcases, is used to plot the P-Delta curve in the immediate vicinity of the jump. Subcases 1 has 1.730 psi, and all subsequent subcases are incremented by 0.01 psi. The Crisfield Arc-Length method is used and the results are plotted in Figure 4. Data for 1.6 psi and 2.0 psi are from the previous runs. This output curve exactly establishes the location of the snap-through jump. It also establishes a continuity in the post-buckling analysis.

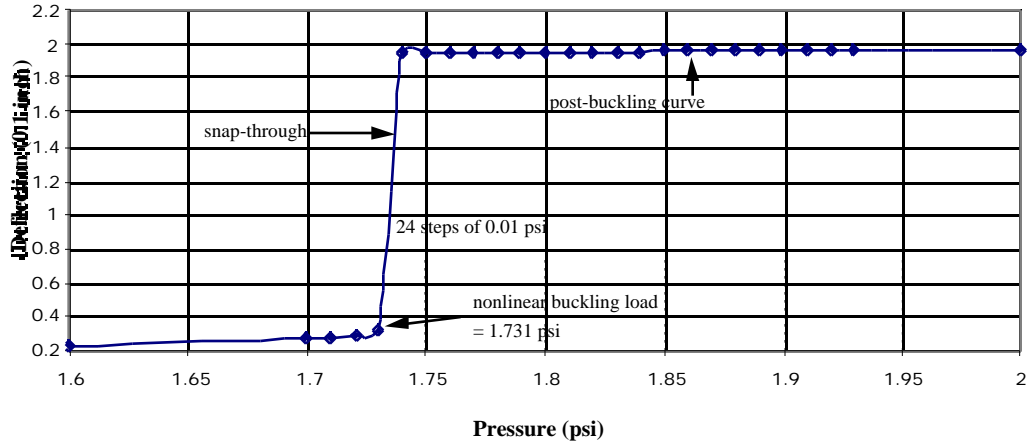


Figure 4: Post-Buckling Analysis by Crisfield's Arc-Length Method

3.5 NASTRAN Runs on Test Structure 2

TS 2 is a flat plate fully fixed at the four edges. The theoretical stresses and deflections based on the curves of Figures 3 and 4a of [2] are calculated as follows:

$$p = \text{Uniform Load} = 10 \text{ psi}$$

$$(b/t) (rp/E)^{-} = (10/.048) (1.0 \times 10/30 \times 10^6)^{-} = 5.005$$

$$p(b/t)^2 = 10 (10/0.048)^2 = 434,000 \text{ psi}$$

From Figure 3 of [2]:

$$t = 2.3 \text{ for } \delta_0/t = 0 \text{ and } (b/t)(rp/E)^{-} = 5.005$$

where δ_0 is the central deflection of plate.

$$\text{Therefore, } \delta_0 = (2.3 \times t) = 2.3 \times .048$$

$$= 0.1104 \text{ in.}$$

From Figure 4a of [2]:

$$f_c/p(t/b)^2 = 0.0478 \text{ for } \delta_0/t = 0 \text{ and } (b/t)(rp/E)^{-} = 5.005$$

where f_c = stress at bottom (unloaded) face at the center of the plate.

$$= [0.0475 (p(b/t)^2)]$$

$$= 0.0475 \times 434,000$$

$$= 206,150 \text{ psi}$$

The NASTRAN printed results for 10 psi are as follows:

$$\text{Central deflection} = 0.1084 \text{ in.}$$

$$\sim 0.1104 \text{ in. theoretical deflection}$$

$$\text{Error, } e = 1.81 \%$$

Central stress at unloaded face of the plate

$$= 210,340 \text{ psi}$$

~ 206,150 psi theoretical stress

$$e = 2.03 \%$$

3.6 NASTRAN Run on Test Structure 3

TS3 is a curved plate with curved edges simply supported and uniformly loaded. It is intended to simulate panels of aircraft wings, stabilizers, and other airfoil shapes. NASTRAN and the theoretical curves results are correlated as follows:

$$\rho/t = 0.345/0.048 = 0.7187$$

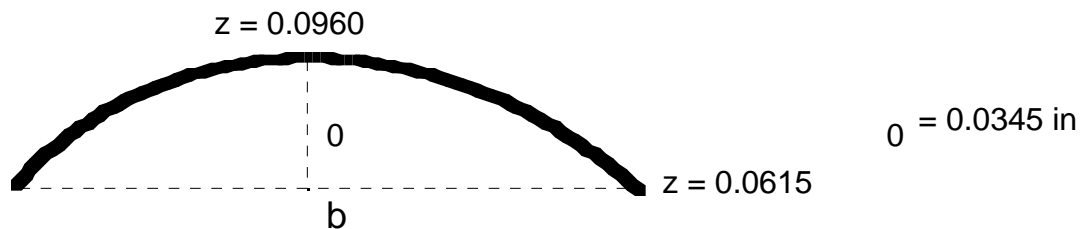


Figure 5 of [2] gives:

$$f/t = 3.32 \text{ at } 10 \text{ psi}$$

Therefore, the central deflection

$$= 3.32 \times 0.048$$

$$= 0.1594 \text{ in.}$$

~ 0.1667 in. NASTRAN value

$$e = 4.58 \%$$

Figure 6a of [2] gives:

$$(f_c/p)(t/b)^2 = 0.053$$

Therefore, f_c the central stress

$$= 0.053 \times 434,000$$

$$= 23,002 \text{ psi}$$

~ 24,490 psi NASTRAN value

$$e = 6.08 \%$$

The NASTRAN run in this section is for a practical aircraft structural panel with curved edges, whereas the theoretical curves are for straight edges. Considering the small percentile errors in stresses and

displacements, it is concluded that the parametric design curves can be used in the preliminary design of aircraft structural panels.

4. PRACTICAL APPLICATION OF NASTRAN

The Aerostructures Corporation at Nashville is currently designing a Leading Edge (L/E) structure, including the D-Nose area for a large commercial airplane. Considering the thin curved panels involved, it is decided to study the nonlinear stability and to detect the presence of a snap-through jump, if any. Since the latter phenomenon is accompanied by a sudden large displacement with a small change in load, a shock wave is generated through the structure. This situation is to be avoided for an appropriate design of the L/E. MSC/NASTRAN Ver 70.0.0 is used for the analysis.

4.1 The Leading Edge Structure

The structural components of the L/E are shown in Figure 5. Starting from the inboard pylon, the L/E section under consideration is 68 feet long between the mid- and outboard areas. The widths at the beginning and end of the section under consideration are 25.47 inches and 14.4 inches respectively. The finite element model is built from the inboard pylon to the tip rib. The structural behavior of this global model indicates a buckling possibility of the L/E skin and rib components between Track 7 (TR7) and Track 8 (TR8). The second location identified is between Track 15 (TR15) and Track 17 (TR17). Thus, from the global model of the L/E, two local models are generated: first, between TR7 and TR8, and second, between TR15 and TR17. The purpose of the analysis is to determine factors of safety against buckling, and also to investigate if the snap-through condition exists.

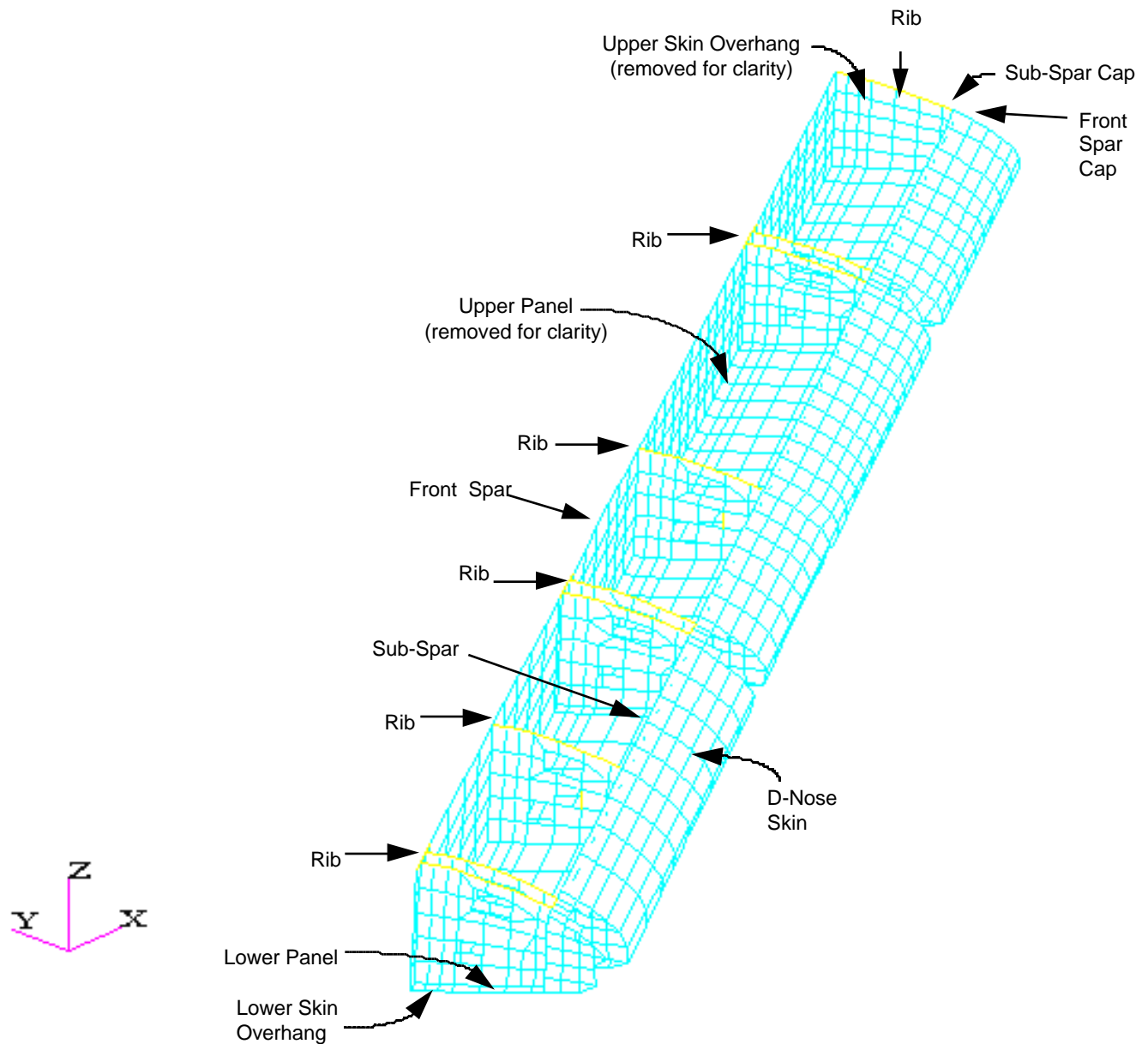


Figure 5: Structural Elements of a Leading Edge

4.2 Finite Element Model

A finite element model of the L/E is built from the inboard pylon to the tip rib. The model includes the built-up representation of the main wing box and L/E components (upper fiberglass panels, lower carbon fiber reinforced plastic panels, track and hold down ribs, sub-spar, and D-Nose skins and riblets).

The main wing box front spar is modeled as beam elements for the upper and lower caps and CQUAD4 elements for the web. The sub-spar upper and lower caps are modeled as rods to transmit only axial loads and torques. The sub-spar web is modeled as CQUAD4 elements. The fiberglass upper panels, carbon fiber reinforced plastic lower panels, and D-Nose skins and riblets are CQUAD4 elements. Discontinuities in the D-Nose at the track and hold down ribs are properly represented. The attachment

between the upper skin of the main wing box and the L/E skin panel is represented by CELAS2 spring elements with proper fastener diameters.

The first local model (between TR7 and TR8) is fixed at the main spar and loaded uniformly with a downward normal load to the top skin. NASTRAN nonlinear analysis SOL 106 is used. Large displacement theory is initiated using a PARAM, LGDISP card. In the preliminary run, the load is incremented from zero to 10 psi at 1 psi intervals. It is observed that an eigenvalue occurs between 5 and 6 psi. Smaller load increments are used in the eigenvalue extraction restart run. Two buckling modes are detected. The corresponding buckling loads are calculated using Equation (2.2) of Section 2.1

The second local model (between TR15 and TR17) is converged up to the 7.50 psi step only, and no buckling mode is detected. No further attempt is made to carry out the analysis beyond this load because of a large reserved factor of safety calculated at this finally converged load step.

4.3 Analysis Results

A load step of 0.01 psi is used in the restart run of the first local model. Two eigenvalues are extracted. The lowest buckling mode is observed at 5.54 psi, giving a factor of safety of 2.20 against buckling. The P-Delta curves are plotted in Figure 6 for linear and nonlinear analyses. The deflection contour for the upper skin is shown in Figure 7. No snap-through jump is detected even with the small load increment of 0.01 psi in the vicinity of the buckling load. The P-Delta curve is continuous and smooth as shown in Figure 6 below.

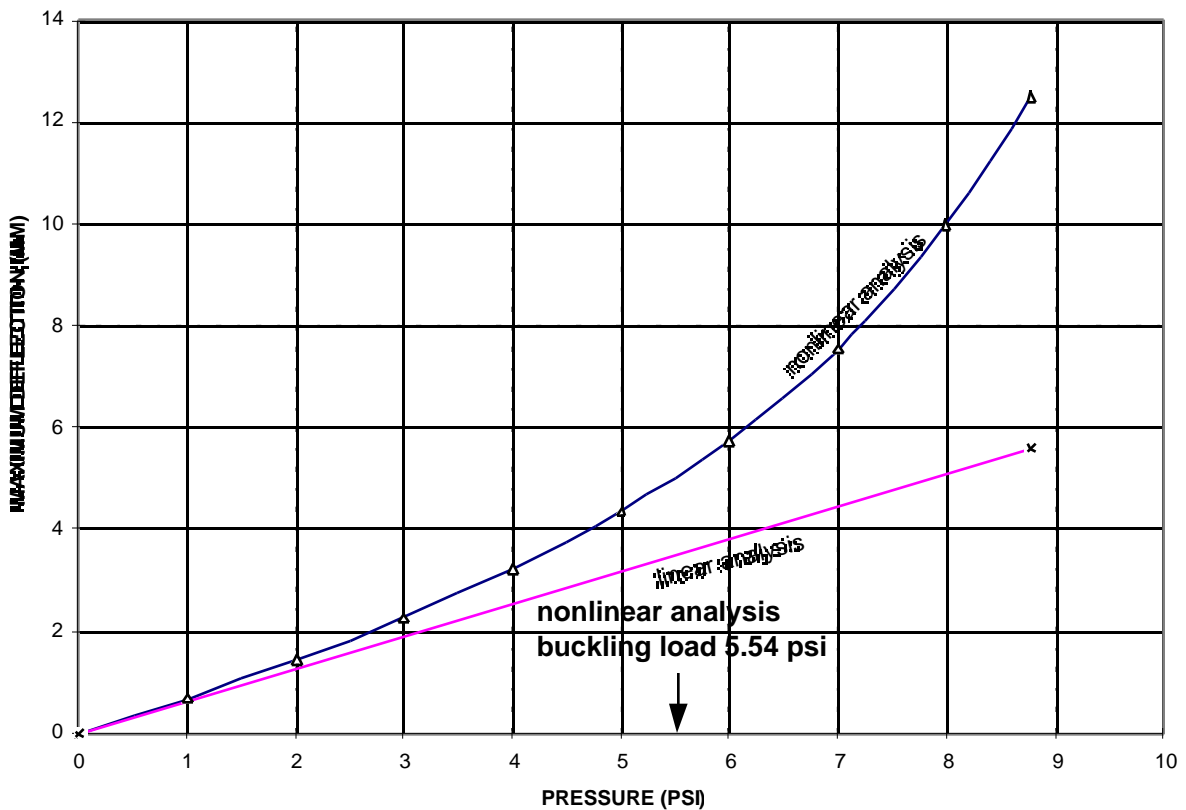


Figure 6: Nonlinear Buckling Analysis of L/E and D-Nose Section Between TR7 and TR8

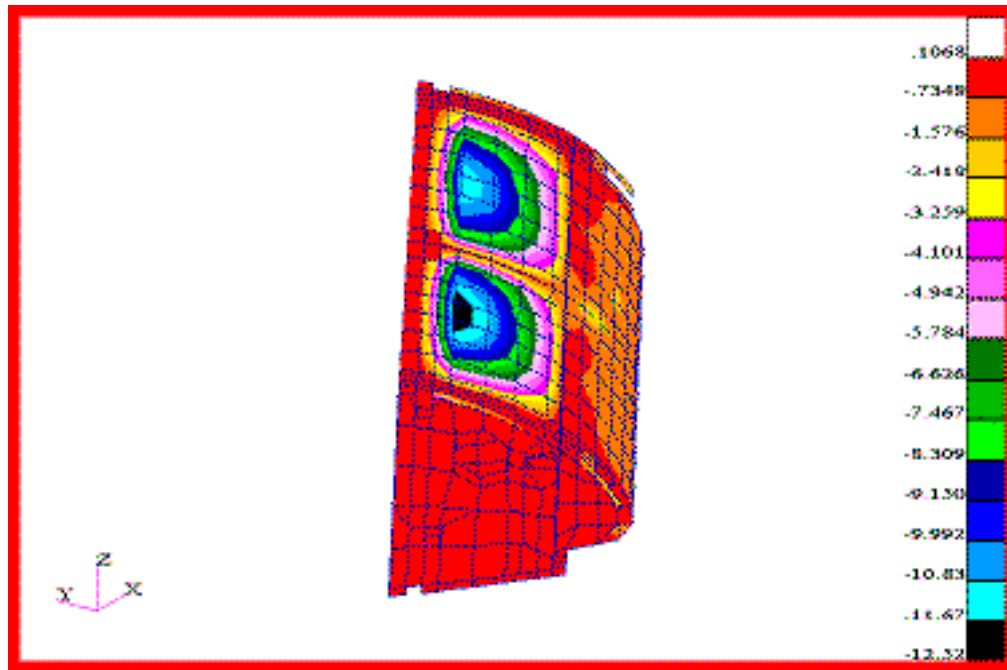


Figure 7: Displacement Fringes of Top Skin Between TR7 and TR8

The second local model is given in Figure 8. The P-Delta curve for the linear and nonlinear analyses is shown in Figure 9, and the skin contour plot of deflections is presented in Figure 10. The factor of safety against buckling is greater than 2.5 and no snap-through phenomenon is observed.

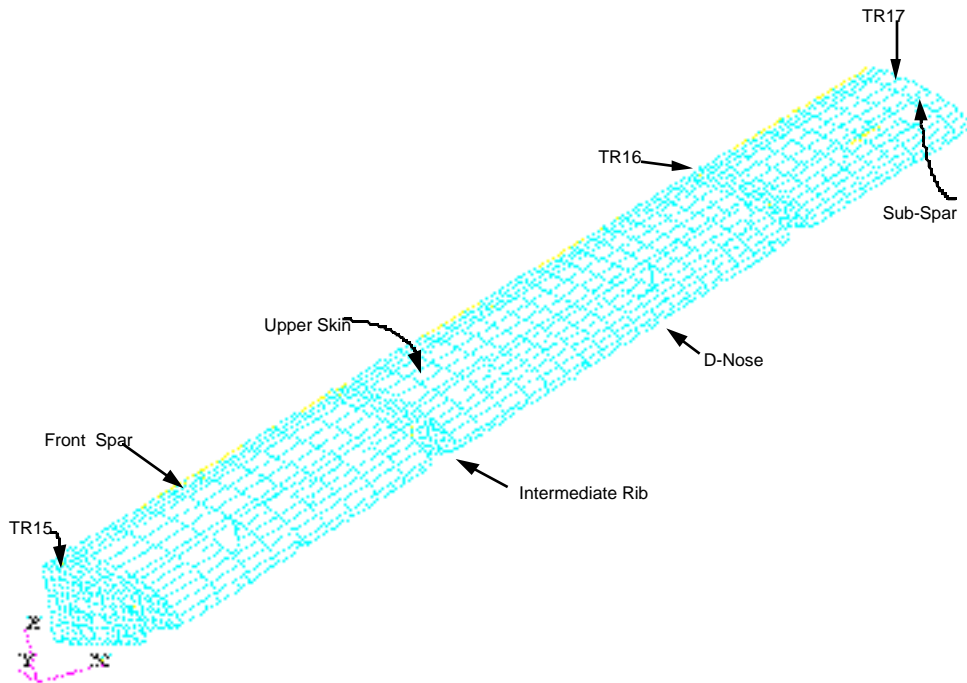


Figure 8: Finite Element Model of L/E and D-Nose Section Between TR15 and TR17

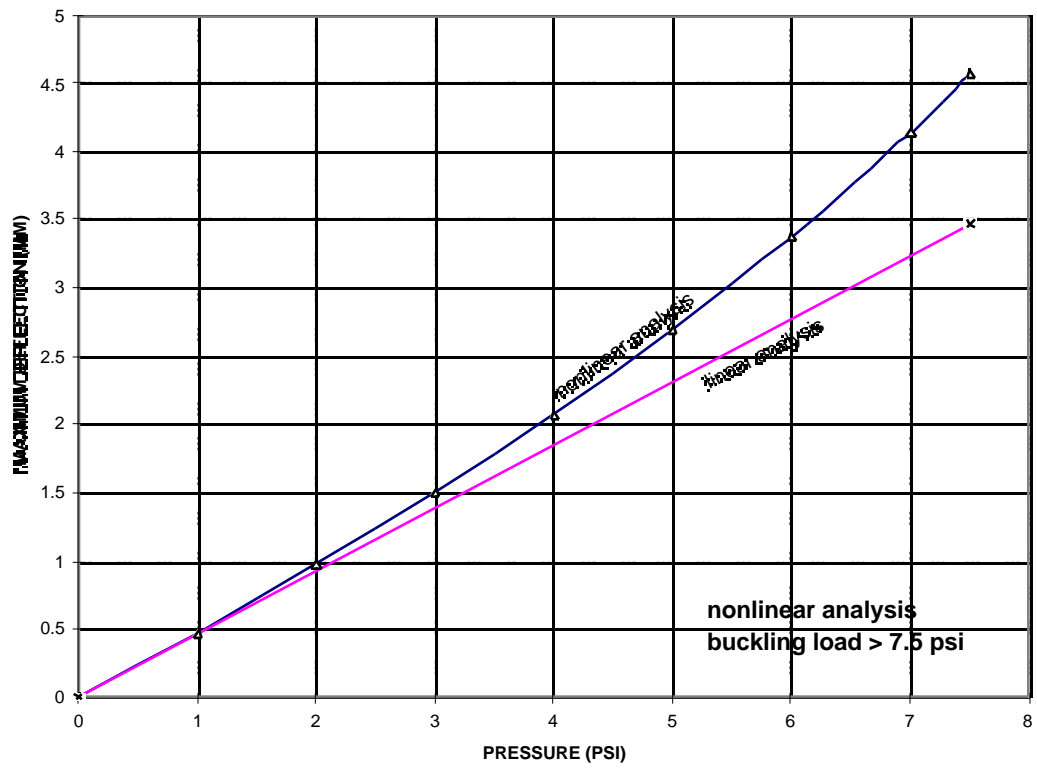


Figure 9: Nonlinear Buckling Analysis of L/E and D-Nose Section Between TR15 and TR17

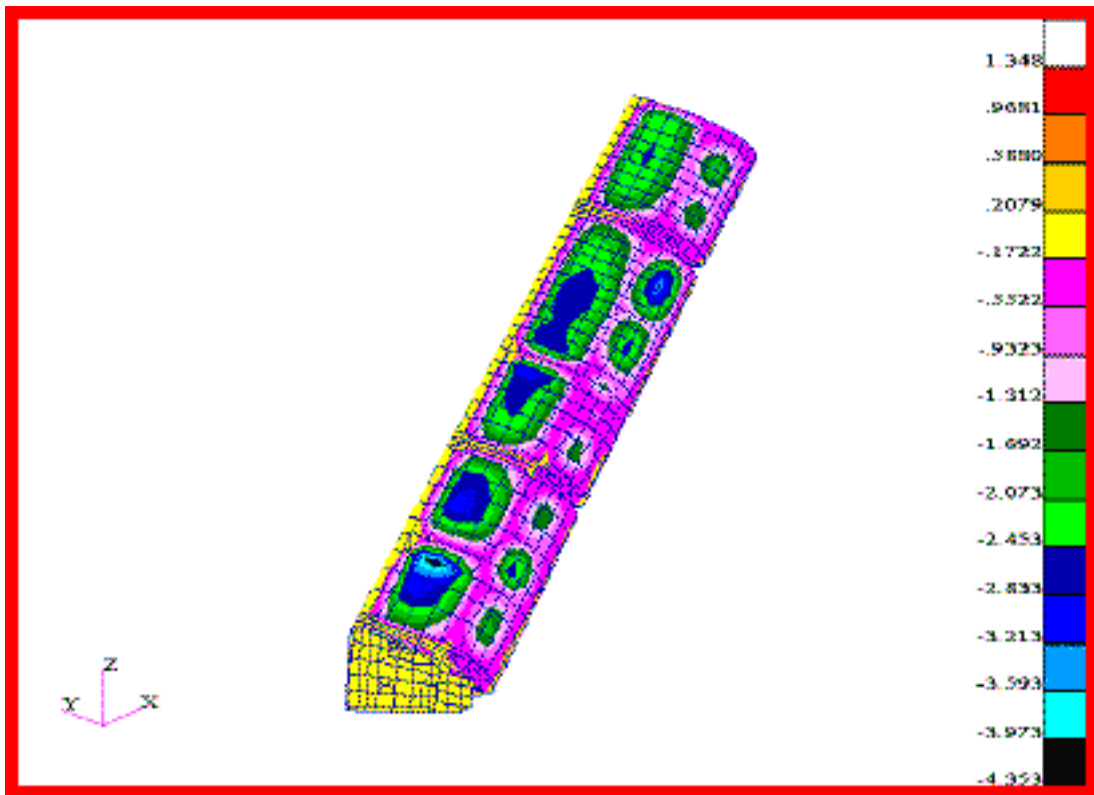


Figure 10: Displacement Fringes of Top Skin Between TR15 and TR17

5. CONCLUSIONS AND RECOMMENDATIONS

The snap-through buckling procedure of MSC/NASTRAN is validated using the well established closed form solution presented in [1]. Excellent correlation is observed for the displacements, stresses, and buckling loads. The procedure is found useful to design a large scale practical structure, such as a leading edge of a commercial airplane.

The parametric curves given in [2] for straight edge panels can be used for a preliminary design of the curved edge aircraft structural panels such as of a wing, leading edge, or empennage. The procedure is given in Section 3.6 of this paper.

It is recommended that the nonlinear buckling analysis be made more user friendly. The necessity of updating the stiffness matrix at least twice before eigenvalue extraction should be satisfied by an internal algorithm. The current error message in this case is somewhat vague and ambiguous.

It may be possible to detect the presence of a snap-through jump by tracking the slope of the P-Delta curve at the maximum deflection grid. The load increments can then be adjusted internally to trace the jump. The current iteration scheme can miss the jump by smoothing the curve in the jump's vicinity unless the special procedure is followed to trace it.

ACKNOWLEDGEMENTS

The author wishes to acknowledge Messrs. Tim Harris, Mike Giblin, Frank Doyal, Glen Sherwin, and Sudhakar Reddy of The Aerostructures Corporation for giving him the opportunity to work on this paper. The author also expresses his sincere thanks to Ms. Marthe' Cumming of Aerostructures for her editing assistance and to Ms. Trish Autery of Aerostructures for typing the manuscript.

REFERENCES

- [1.] Timoshenko, P.S., and Woinowsky-Krieger, S., *Theory of Plates and Shells*, 2nd. ed., McGraw-Hill, 1959.
- [2.] "Elastic Stresses and Deflections for Square Plates with Small Initial Curvature Under Uniform Pressure on Concave or Convex Face", *ESDU International*, December, 1987.
- [3.] *MSC/NASTRAN Handbook for Nonlinear Analysis*, Version 67, The MacNeal-Schwendler Corporation, Los Angeles, CA March 1992.